AD-A061 020 AIR FORCE GEOPHYSICS LAB HANSCOM AFB MASS F/G 17/5

CALIBRATION OF THE HI STAR SENSORS.(U)

JUL 78 S D PRICE, R G WALKER

UNCLASSIFIED AFGL-TR-78-0172 NL

1 OF 1

AD A061 020

END

DATE FILMED

2-79

DDC

AFGL-TR-78-0172
INSTRUMENTATION PAPERS, NO. 268

Calibration of the HI STAR Sensors

STEPHAN D. PRICE
RUSSELL G. WALKER

3 July 1978

Approved for public release; distribution unlimited.

OPTICAL PHYSICS DIVISION PROJECT 7670
AIR FORCE GEOPHYSICS LABORATORY
HANSCOM AFB, MASSACHUSETTS 01731

AIR FORCE SYSTEMS COMMAND, USAF

This report has been reviewed by the ESD Information Office (OI) and is releasable to the National Technical Information Service (NTIS).

This technical report has been reviewed and is approved for publication.

FOR THE COMMANDER

John Harwood

Chief Scientist

Qualified requestors may obtain additional copies from the Defense Documentation Center. All others should apply to the National Technical Information Service.

Unclassified

SECURITY CLASSIFICATION OF THIS PAGE (When Data Entered)

REPORT DOCUMENTATION PAGE		READ INSTRUCTIONS BEFORE COMPLETING FORM
1. REPORT NUMBER AFGL-TR-78-0172, AFGL-IP-268	2. GOVT ACCESSION NO.	3. RECIPIENT'S CATALOG NUMBER
4. TITLE (and Subtitle) CALIBRATION OF THE HI STAR SENSORS.		5. TYPE OF REPORT & PERIOD COVERED Scientific. Interim.
		6. PERFORMING ORG. REPORT NUMBER IP No. 268
7. AUTHOR(s) Stephan D. Price, Russell G. Walker*		8. CONTRACT OR GRANT NUMBER(s)
9. PERFORMING ORGANIZATION NAME AND ADDRESS Air Force Geophysics Laboratory (OPI) Hanscom AFB Massachusetts 01731		10. PROGRAM ELEMENT, PROJECT, TASK AREA & WORK UNIT NUMBERS 62101F 76700606
11. CONTROLLING OFFICE NAME AND ADDRESS Air Force Geophysics Laboratory (OPI) Hanscom AFB Massachusetts 01731		12. REPORT DATE 3 July 1978
		13. NUMBER OF PAGES 30
14. MONITORING AGENCY NAME & ADDRESS (if different from Controlling Office) Instrumentation papers,		15. SECURITY CLASS. (of this report) Unclassified
		15a. DECLASSIFICATION/DOWNGRADING SCHEDULE

16. DISTRIBUTION STATEMENT (of this Report)

Approved for public release; distribution unlimited.

(12) 49p.

DDC RECEIVED NOV 8 1978 B

17. DISTRIBUTION STATEMENT (of the abstract entered in Block 20, if different from Report)

18. SUPPLEMENTARY NOTES

*Present Address: NASA Ames Research Center, Moffett, CA 94035

19. KEY WORDS (Continue on reverse side if necessary and identify by block number)

20. ABSTRACT (Continue on reverse side if necessary and identify by block number)

Problems exist in calibrating a cryogenically cooled infrared sensor system in the laboratory. Although there are limited laboratory facilities which attempt to simulate the actual operational environment, the sensor-tester interface has created difficulties for calibrating LWIR sensors in general. The procedures used to calibrate the AFGL infrared celestial survey experiments are described in detail. It was found that stars are reliable calibration sources which offer several advantages over laboratory references. The long

→ next page

DD FORM 1 JAN 73 1473 EDITION OF 1 NOV 65 IS OBSOLETE

Unclassified

SECURITY CLASSIFICATION OF THIS PAGE (When Data Entered)

409 578

78 10 26 032

LB

Unclassified

SECURITY CLASSIFICATION OF THIS PAGE(When Data Entered)

20. Abstract (Continued)

term stability of the sensor systems as well as linearity of the system are discussed.

RE: Classified references, distribution unlimited-
No change per Mr. B. Schurin, AFGL/OPI

ACCESSION for		
NTIS	White Section	☑
DDC	Buff Section	☐
UNANNOUNCED		☐
JUSTIFICATION		
BY		
DISTRIBUTION/AVAILABILITY CODES		
Dist.	AVAIL. and/or	SPECIAL
A		

Unclassified

SECURITY CLASSIFICATION OF THIS PAGE(When Data Entered)

Contents

Illustrations

Illustrations

Tables

Calibration of the HI STAR Sensors

1. INTRODUCTION

The survey data compiled into the "AFGL Four Color Infrared Sky Survey" catalog[1] were calibrated against selected stars observed during the course of the scan and augmented, when necessary, with relative responsivities measured in the laboratory. The celestial sources used for calibration were chosen from a list, compiled at AFGL, of objects with infrared observations reported in the astronomical literature prior to mid 1974. Subjective judgement was used in selecting the most reliable sources and measurements from the list.

A detailed description of the experimental profile and instrumentation is given by Price and Walker[1] for the nine rocket flights on which survey data were obtained. Briefly, the survey used small (16.5 cm diameter) doubly folded Gregorian telescopes cooled to cryogenic temperatures. The focal plane of each telescope contained three linear staggered arrays of eight detectors each arranged in the cross scan direction and spectrally band limited with interference filters. The sensor scan resulted in sequential observations in the three spectral colors. The cross

(Received for publication 3 July 1978)

1. Price, S.D., and Walker, R.G. (1976) The AFGL Four Color Sky Survey: Catalog of Observations at 4.2, 11.0, 19.8 and 27.4 μm, AFGL-TR-76-0205, Environmental Research Papers, No. 576.

scan field-of-view of adjacent detectors in a single color band overlapped at least optical one blur diameter.

The telescopes used for the first seven experiments were filtered for the 4, 11 and 20 micron spectral regions and used doped Germanium detectors. Silicon detectors were substituted for the last two experiments and a spectral band centered at 27 microns was used in place of the 4 micron color. The same sensor system was flown on the first six experiments and different telescope and/or focal plane was employed for the last three.

A linear regression with fixed unit slope of the observed system magnitudes against the reference magnitudes was performed for each of the 24 detectors on each flight. The preliminary calibrations on the first six experiments, which used the same sensor, indicated that data from the separate flights could safely be combined to improve the accuracy of the calculations. This sensor was also twice calibrated in the MARK 7 chamber at Arnold Engineering Development Center (AEDC). The first test[2] was performed before the survey experiments began and the second[3] was done after the sixth flight. Inconsistances in the data from the first test obviated the use of these results. The data from the second test indicates the presence of systematic errors in the aperature sizes assumed by AEDC for the blackbody integrating cavity. However, the excellent agreement between the second AEDC calibration and that obtained from the stars indicates that these errors were small.

There were an insufficient number of reference stars observed to reliably calibrate each of the detectors for each of the remaining three flights. The reference list for these flights was, therefore, augmented with the results reduced from the previous experiments. Even this was inadequate in some cases, especially for the 27 μm color. For these channels, the relative responsivities of the detectors in each color measured in the laboratory for the focal plane alon[illegible]d to the available celestial reference values. The internal consistency [illegible]dure was found to be good.

---

2. Hickey, R.F. (1971) Performance Evaluation of the SAMSO/Hughes HI STAR Sensor, AEDC-TR-71-63 (Classified Report).
3. Nutt, K.W. (1973) Performance Evaluation of the HI STAR Sensor Using a New Integrating Sphere Target Source, AEDC-TR-73-142 (Classified Report).

2. APPROACH

The voltage output of a linear system due to a spectral irradiance H_λ is given by

$$VR^{-1} = \int_0^\infty S_\lambda H_\lambda \, d\lambda \tag{1}$$

where S_λ is the system spectral response and R its responsivity in terms of volt/watt. These quantities are routinely measured in the laboratory for the focal plane assembly alone. Invariably, the laboratory calibration sources are chopped blackbodies of "known" temperature which flood the full field of the detectors. Thus, not only do optical and electronic transfer functions have to be adopted to convert the measured focal plane response to a system response, but also an equivalence must be assumed between the chopping and scanning frequencies and the illumination geometry of the laboratory sources and those of scanned point-like celestial sources. Sayre et al[4] have measured large variation in responsivity with illumination geometry for the types of detectors used for the AFGL survey.

The stars offer several advantages as infrared calibration sources. The entire system is calibrated during data taking with the actual point source scan geometry and with sources which, for the majority of cases, have spectral characteristics similar to that of the cataloged object. Variations in responsivity over the surface of a detector are averaged out as the stellar transit positions are not fixed. Further, for practical considerations, stars provide the only reliable calibration for spectral bands such as the 4 micron band. This filter has a two micron wide spectral leak of about 4 percent peak transmission at 14 μm. Below 250°K the blackbody energy through this "red" leak is at least as great as the flux in the pass-band. Thus, small errors in the detailed knowledge of the transmission in this leak produce large errors in the correction terms required at these temperatures. Unfortunately, the AEDC[2, 3] calibrations used blackbodies with temperatures on the order of 250°K. The known, and measured, higher temperature of the reference stars reduce the amount of the red leak correction for these sources to less than one percent.

On the other hand, few stars have been measured with sufficient spectral detail in the infrared to allow an exact evaluation of the integral in Eq. (1). Just as for the laboratory sources, some assumptions are necessary concerning their spectral

---

4. Sayre, C., Arrington, D., Eisenman, W., and Merriam, J. (1976) Characteristics of Detectors Having Partially Illuminated Sensitive Areas, IRIS Meeting on Detectors.

distributions. Also, there are too few true astronomical photometric standard stars bright enough to reliably calibrate each of the detectors for each experiment, so measurements on stars of late spectral type, that is, cool, small amplitude and Mira type variable stars had to be included in the list of reference sources. The variability of these stars is much smaller in the infrared than the visual, often amounting to only 10 to 20 percent.

The spectral characteristics of a system may be expressed by the system unique parameters of effective wavelength, designated λ_e, and effective bandwidth, $\Delta\lambda_e$. These quantities are defined by

$$\lambda_e \equiv \int_0^\infty \lambda S_\lambda \, d\lambda \Big/ \int_0^\infty S_\lambda \, d\lambda \tag{2a}$$

and

$$\Delta\lambda_e = \int_0^\infty S_\lambda \, d\lambda \tag{2b}$$

respectively. Table 1 lists these quantities for the instruments used for the AFGL Infrared Sky Survey.

Table 1. Effective Wavelength and Bandwidths for the Survey Sensors

Hi Star		Hi Star South	
λ_e (μm)	$\Delta\lambda_e$ (μm)	λ_e (μm)	$\Delta\lambda_e$ (μm)
4.16	1.50	11.11	5.67
11.00	5.14	19.63	5.99
19.80	5.59	27.43	3.44

Expanding the irradiance in Eq. (1) about the effective wavelength, we get[5]

$$H_\lambda = H_{\lambda e} + \left.\frac{dH}{d\lambda}\right|_{\lambda_e} (\lambda - \lambda_e) + \frac{1}{2} \left.\frac{d^2H}{d\lambda^2}\right|_{\lambda_e} (\lambda - \lambda_e)^2 + \cdots + \frac{1}{\eta!} \left.\frac{d^\eta H}{d\lambda^\eta}\right|_{\lambda_e} (\lambda - \lambda_e)^\eta$$

thus

$$VR^{-1} = \left\{ H_{\lambda e} + \frac{1}{2} \left.\frac{d^2H}{d\lambda^2}\right|_{\lambda_e} f_2(\lambda_e) + \cdots + \frac{1}{\eta!} \left.\frac{d^\eta H}{d\lambda^\eta}\right|_{\lambda_e} f_\eta(\lambda_e) \right\} \int_0^\infty S_\lambda \, d\lambda \qquad (3)$$

where

$$f_\eta(\lambda_e) = \int_0^\infty (\lambda - \lambda_e)^\eta S_\lambda \, d\lambda \Big/ \int_0^\infty S_\lambda \, d\lambda$$

and $f_1(\lambda_e) = 0$ from the definition of λ_e.

Equation (4) may be written

$$VR^{-1} = H_{\lambda e} \, \Delta\lambda_e \, (1 + \Delta H) \qquad (4)$$

where ΔH is the color correction term which involves the second and higher order terms in the expansion. This is an exact expression equating the integrated in-band irradiance, and hence the system response, to the monochromatic irradiance at the effective wavelength of the spectral band of the system, $H_{\lambda e}$, times the respective bandwidth through a proportionality constant ΔH, a color correction term. For the spectral bands used on the AFGL Survey, ΔH is about 0.25 for a λ^{-4} infrared spectral distribution and less for flatter variations with wavelength.

The photometry on the reference sources is in terms of magnitude, a logarithmic relationship between the stellar irradiance and that from a standard source. The adopted standard source is an AOV star at a distance of 10 parsecs (3.1×10^{19} cm). The infrared energy distribution from such a star can be accurately represented by a 10,000°K blackbody radiator which subtends 1.5697×10^{-16} steradians. The magnitude of a star at λ_e is defined by

5. Stromgren, B. (1937) Handbuch der Experimental Physik, ed. Wein and Harms, Leipzig: Akademishe Verlags Gesellschaft M.B.H., 26:321.

$$m_s(\lambda_e) = -2.5 \log \left| \frac{H_{\lambda e}(s)}{H_{\lambda e}(AOV)} \right| .$$

The observed system magnitude is defined as

$$m_o = -2.5 \log \left\{ \frac{\int_o^\infty H_\lambda(s) S_\lambda \, d\lambda}{\int_o^\infty H_\lambda(AOV) S_\lambda \, d\lambda} \right\} \tag{5}$$

which can be expressed in terms of the responsivity from Eq. (1) as

$$= -2.5 \log VR^{-1} + C_o . \tag{6}$$

Here C_o is the logarithm of the integrated zero point flux of the system and is uniquely determined for each color.

Employing the relationship given in Eq. (4), Eq. (5) can also be rewritten

$$m_o = -2.5 \log \left| \frac{H_{\lambda e}(s) \, \Delta\lambda_e \, (1 + \Delta H(s))}{H_{\lambda e}(AOV) \, \Delta\lambda_e \, (1 + \Delta H(AOV))} \right|$$

$$m_o = -2.5 \log \left| \frac{H_{\lambda e}(s)}{H_{\lambda e}(AOV)} \right| -2.5 \log \left| \frac{1 + \Delta H(s)}{1 + \Delta H(AOV)} \right| \tag{7}$$

$$m_o = m_s(\lambda_e) + C_1 . \tag{8}$$

Equating (6) and (8) and rearranging terms, we have

$$2.5 \log V = -m_s(\lambda_e) + 2.5 \log R + C_o - C_1 . \tag{9}$$

V is the measured variable, voltage, $m_s(\lambda_e)$ is the reference magnitude input, R is the sought for system responsivity, C_o is a known system value and C_1 is a constant which contains an unknown color correction term. Noting that

$$C_o - C_1 = 2.5 \log \left\{ \int_0^\infty H_\lambda(AOV)\, S_\lambda \, d\lambda \right\} + 2.5 \log \left\{ \frac{1 + \Delta H(s)}{1 + \Delta H(AOV)} \right\}$$

$$= 2.5 \log \left[H_{\lambda e}(AOV)\, \Delta\lambda_e \,(1 + \Delta H(AOV)) \left\{ \frac{1 + \Delta H(s)}{1 + \Delta H(AOV)} \right\} \right]$$

$$C_o - C_1 \simeq 2.5 \log \left\{ H_{\lambda e}(AOV)\, \Delta\lambda_e \right\} + \Delta H(s)$$

$$\text{if } \Delta H(s) \le 0.3 \quad . \tag{10}$$

Equation (9) may be rewritten in terms of the monochromatic zero point flux:

$$2.5 \log V = -m_s(\lambda_e) + 2.5 \log R + 2.5 \log \left\{ H_{\lambda e}(AOV)\, \Delta\lambda_e \right\} + \Delta H(s) \quad . \tag{11}$$

A reference star with a known magnitude at λ_e can be used to determine the system responsivity to within a constant ΔH by means of Eq. (11). If the stars used in the calibration have similar infrared energy distributions, then their color corrections terms are approximately the same and average calibration may be obtained to within a mean color correction value representative of the class of objects used. The star to star differences in color correction terms then introduces scatter into the calculations.

Almost all the reference stars are cool giant or supergiant stars with photospheric effective temperatures between 2000 and 3500°K. Many of these stars possess circumstellar emission which enhance the flux in the ten micron region by as much as a factor of three. For "oxygen" stars the emission feature is due to silicate grains. In "carbon" stars the enhancement is caused by silicon carbide plus an underlying continuum with characteristic temperatures on the order of 600°K. Detailed studies by Merrill[6] and Forrest et al[7] on a number of the objects in the reference list show that the infrared energy distributions for these stars are smooth and somewhat similar, and that over the spectral bands used for the survey the energy distributions are either proportional to λ^{-4} for the photospheric radiators or somewhat flatter if circumstellar emission is contained in the band. Thus, for the system bands ΔH varies from zero for an equal energy distribution to about 0.25 for λ^{-4} distribution. This implies that the approximation used in Eq. (10) is

---

6. Merrill, K.M. (1977) Infrared Observations of Late Type Stars, Invited Review Paper at I.A.V. Symposium No. 42.

7. Forrest, W.J., Gillett, F.C., and Stein, W.A. (1975) Circumstellar grain and the intrinsic polarization of starlight, Ap. J. 195:423.

valid for the reference list stars and the star to star color correction differences will be small second order terms.

It now remains to transfer the reference magnitudes from the astronomical literature to values at the system effective wavelengths. The λ_e (4.2 μm) reference magnitudes were obtained by either interpolating linearly in magnitude between published values at 3.5 μm and 5 μm or, if there is no 5 μm reference values reported, extrapolating the 2.2 μm and 3.5 μm reference values. This procedure is valid if the stellar spectral distribution obeys a power law in wavelength through this region, an applicable assumption for the reference list sources. A small systematic error amounting to a few percent for some of the stars may have been introduced due to CO absorption at 4.3 μm.

The various ground based photometric systems which reported stellar measurements in the 8 to 24 micron region have color bands with effective wavelengths at or very close to, that is, within 10 percent, the λ_e (11.0 μm) and λ_e (19.8 μm) system bands. The ground based measurements were adopted directly and errors due to mismatch in the effective wavelength and bandwidths between the ground based and our space borne systems were assumed to introduce random scatter into the calibration. The λ_e (27.4 μm) calibration references will be discussed separately.

The compiled list of reference sources is contained in Appendix A along with the adopted magnitudes at the system effective wavelengths. The maximum and minimum brightness which have been reported are also given. In most cases, the adopted magnitude is a simple mean of the brightness extrema.

Although known infrared variables were accepted as reference sources under penalty of increased scatter, stars known to vary by more than 0.75 magnitudes (a factor of two in brightness) were eliminated from the calibration. Beam size effects were at least partially accounted for by deleting all objects known, or measured by the survey, to be extended.

The reference sources used in the calibrations were further restricted to stars in the IRC.[8,9] This was done to increase the probability that the reference source was indeed a star with no unusual infrared spectral properties or beam size effects.

A linear least squares regression with fixed unit slope of the observed magnitude, more precisely 2.5 times the logarithm of the observed voltage, against the reference magnitudes is calculated. The solution intercept at $m_s(\lambda_e) = 0$ leads directly to the system responsivity through Eq. (11).

---

8. Neugebauer, G., and Leighton, R.B. (1969) Two Micron Sky Survey, A Preliminary Catalog, NASA SP-3047.

9. Neugebauer, G. (1971) Unpublished extension to the IRC.

3. RESULTS

The sensors proved to be very stable. The response of the detectors to low temperature, evaporated thin film, infrared emitting sources pulsed during the experiment remained constant to within 10 percent even though the background varied by as much as a factor of five. Furthermore, the preliminary calibrations for the first six experiments which employed the same sensor system had remarkable homogeniety. This agreement is shown in Figures 1 and 2. The reference star magnitudes are plotted against observed magnitudes for two of the λ_e (4.2 μm) channels in Figures 1a and 1b, while Figures 2a and 2b are similar plots for two of the λ_e (11.0 μm) channels. The different symbols on these plots represent different flights. The data from the first six experiments were combined in order to improve the accuracy of the calculations. Note also that the reference sources extend over a factor of 100 (5 stellar magnitudes in the figure) in brightness.

An iterated linear least squares regression with fixed unit slope was calculated for each detector of the logarithm of the observed voltage against the reference magnitude by means of Eq. (11). The intercept of the solution leads directly to the systém responsivity if an average value is adopted for the color correction term. The solutions for each channel were iterated by rejecting as many as five sources with the largest deviations exceeding twice the standard deviation of the previous solution. This was done in order to minimize the effects of any large deviations due to unknown beam size effects, a greater variability of the source than the reference values indicate, or large unknown measurement errors. Also, only measurements on reference sources which exceed a specified signal-to-noise ratio were included in order to minimize the measurement error.

Table 2 lists the least squares calibration parameters based on stellar references for the combined six experiment data compared to other calibration methods. The first column lists the channel number; channels 1 through 8 are filtered for λ_e (11.0 μm), the λ_e (4.2 μm) channels are 9 through 15 (channel 16 was inoperative) and channels 17 through 24 are λ_e (19.8 μm) colors. The number of reference star observations used in calibrating each channel after all rejections is listed in column 3. As expected, the number of reference sources available for calibration decreases with increasing wavelength. Indeed, there were hardly enough sources in the λ_e (19.8 μm) band to permit a meaningful regression calculation.

As a check on the linearity of the system, a separate regression was calculated with the slope as a free parameter. Column 3 gives the value of the derived slope and column 4 lists the root mean square deviation of the fixed unit slope. Over half the channels have slopes within one rms of unity while all but one channel are within two standard deviations. This argues strongly that the system response was indeed linear.

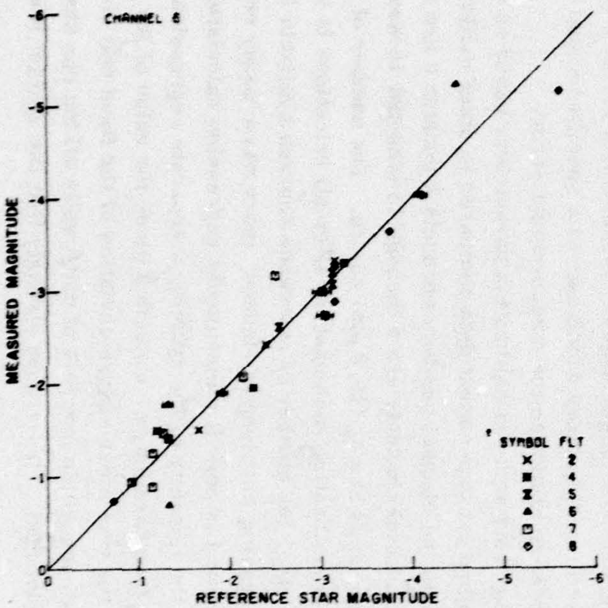

Figure 1a. Comparison of the Measured versus Reference Star Magnitudes for a λ_e (4.2 μm) Channel. The different symbols for the data points represent the preliminary calibrations for the individual experiments for the first six flights which used the same sensor system. The horizontal lines in the figure represent the range of values found for the reference source.

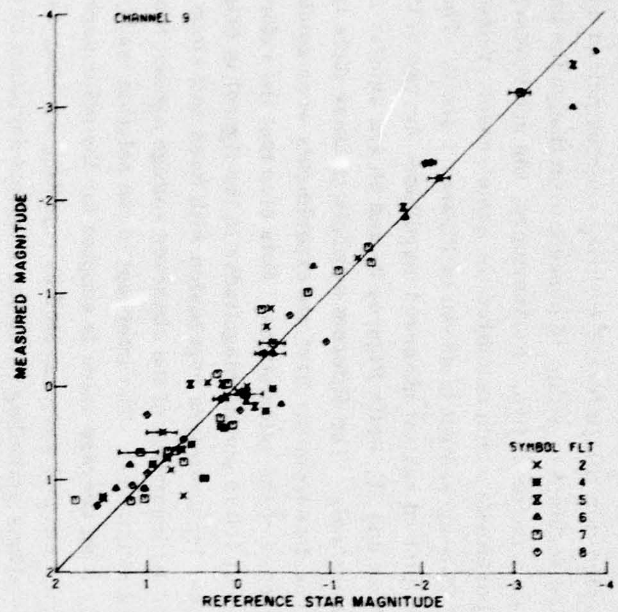

Figure 1b. Comparison of the Measured versus Reference Star Magnitudes for a Different λ_e (4.2 μm) Channel. The different symbols for the data points represent the preliminary calibrations for the individual experiments for the firxt six flights which used the same sensor system. The horizontal lines in the figure represent the range of values found for the reference source

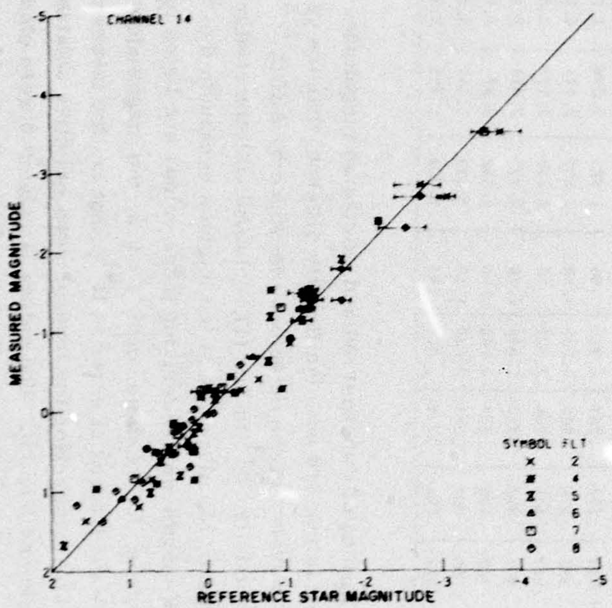

Figure 2a. Comparison of the Measured versus Reference Star Magnitudes for the Most Sensitive λ_e (11.0 μm) Channel. *The different symbols for the data points represent the preliminary calibrations for the individual experiments for the first six flights which used the same sensor system.* The horizontal lines in the figure represent the range of values found for the reference source

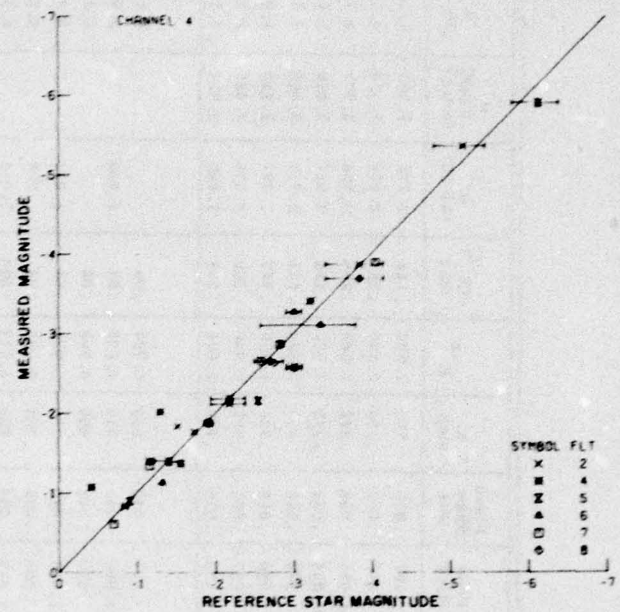

Figure 2b. Comparison of the Measured versus Reference Star Magnitudes for a Different λ_e (11.0 μm) Channel. The different symbols for the data points represent the preliminary calibrations for the individual experiments for the first six flights which used the same sensor system. The horizontal lines in the figure represent the range of values found for the reference source.

Table 2. Comparison of the Calibration Parameters Obtained With Stellar References and Values Derived From Independent Sources

Channel No. λ_e(11 μm)	No. of Stars	Free Slope	Fixed Slope rms	σ mag	R^{-1}	$\sigma(R^{-1})$ mag	R^{-1} (AEDC)	R^{-1} (AEDC Noise)	R^{-1} (Wake)	R^{-1} (Diode)
1	37	.897	.056	.315	2.988	.144	3.274	2.890	3.087	2.907
2	18	.959	.087	.294	5.294	.23	3.949	5.530	5.260	5.922
3	31	1.015	.094	.372	2.589	.216	3.098	2.993	2.71	2.065
4	25	1.054	.054	.329	3.976	.153	3.517	2.540	3.69	3.05
5	31	.973	.056	.294	2.632	.131	2.723	2.899	2.53	2.53
6	37	.990	.069	.354	1.820	.167	1.971	2.455	1.82	1.77
7	22	.887	.085	.363	2.020	.203	3.050	3.586	2.55	3.11
8	30	.805	.079	.430	2.074	.217	1.689	2.934	2.74	2.58
λ_e(4.2 μm)										
9	79	.877	.040	.359	5.797	.04			4.663	5.725
10	59	1.086	.043	.319	6.652	.04	1.958		3.996	4.117
11	41	.899	.063	.400	6.352	.06			3.176	6.808
12	71	1.005	.042	.350	5.924	.04	1.074		2.373	5.544
13	47	.996	.043	.294	4.055	.04	.793		4.244	7.332
14	72	1.019	.035	.288	4.573	.035	1.911		4.52	4.483
15	75	1.044	.044	.380	5.620	.04	1.132		3.85	3.698
λ_e(19.8 μm)										
17	8	.984	.093	.245	2.782	.45	2.212	2.538	2.646	2.807
18	7	1.042	.193	.287	1.715	.50	1.923	2.028	1.763	2.022
19	6	.553	.316	.443	3.395	1.30	2.857	2.471	4.381	3.26
20	6	.947	.151	.256	2.663	.70	2.447	2.710	2.313	2.43
21	4	.981	.290	.415	2.856	1.30	2.773	2.824	2.615	2.23
22	6	.762	.130	.357	1.792	.56	2.382	2.27	1.913	2.26
23	7	.600	.305	.531	2.626	1.19	2.422	2.649	4.32	2.79
24	9	.861	.094	.274	2.429	.43	2.054	1.867	1.72	2.47

The standard deviations of the observed and calculated magnitudes are given in column five. These values are not significantly different than the variations in responsivity over the surfaces of the detectors measured by AEDC.[2,3]

The inverse responsivity, R^{-1} in Eq. (1), obtained with the stellar calibration references and normalized to unit power of ten is given in column 6 of Table 2 and the error, in terms of magnitude, in deriving these values are listed in column 7. For small values of error, for example, $\sigma(R^{-1}) < 0.3$, the magnitude error is approximately equal to the fractional error in R^{-1}, that is, the inverse responsivity is $R^{-1}(1 \pm \sigma(R^{-1}))$. For comparison the inverse responsivities obtained from AEDC tests[3] are listed in columns 8 and 9. The values in column 8 were obtained by a linear least square fit of the measured voltage to a "known" irradiance from a point

source transitting a detector at the nominal survey rate. The source always transited the detectors at the same specified elevation so these values are not averaged over the detector's surface. The AEDC data[3, 10] indicate that there may be a small systematic error of 5 to 15 percent in the adopted values of the blackbody aperature sizes. The standard deviations of the observations to the linear fit for the λ_e (11 μm) values in column 8 are between 6 and 36 percent and are comparable to the equivalent values of $\sigma(R^{-1})$ based on the stars. The λ_e (4.2 μm) AEDC data have large discrepancies which are certainly due to the red leak in this filter.

The inverse responsivities in column 9 were obtained at AEDC by measuring the mean square noise voltage as a function of a controlled, known background. The measurement errors are bound to be somewhat high as the measured voltage changes with the square root of the photon flux, making the measurement insensitive to changes in the input variable and restricting the measurements to only three or four points because of dynamic range considerations. Despite these factors, the two calibrations are within 30 percent of each other for all but three channels. Again, the red leak in the λ_e (4.2 μm) channel precluded meaningful measurements by this technique.

The last two columns contain relative inverse responsivities, scaled to the values obtained from the stars, derived from transient phenomena which fill the field-of-view of each detector and were observed on each flight. These values were included in order to evaluate possible independent measurement methods which could be used to derive the relative detector responses and to check possible geometry effects. Column 10 lists the relative inverse responsivities derived from observations made on the high altitude re-entry wake of the rocket sustainer. As this phenomenon was of significant angular extent, the desired information was derived by extending the system response toward dc by applying the inverse bilinear z transform of the electronic high pass filter to the data stream. The resulting spatial energy distributions were well represented by Gaussian profiles. The internal consistency of the resulting amplitudes were between 5 and 13 percent of the scaled mean. The amplitude, flux and width of this phenomena are observed to change from scan to scan over a period of nine seconds,[11] and a time dependence is expected during a single observation in the sense that the bottom detectors of the array observe excited air from a shock which was formed a fraction of a second more recently than the top ones. This effect cannot be large as the measured half widths are well within the measurement error for all channels on a single scan and no systematic variation is evident. The λ_e (11 μm) and λ_e (19.8 μm) inverse

---

10. Hiatt, J. (1975) ARPA/Perkin-Elmer MARK VII Sensor Test, AEDC-TR-75-50 (Classified Report).

11. Murdock, T. L., and Walker, R. G. (1975) Infrared Signatures of High Altitude Reentry Wakes, AFCRL-TR-75-0083 (Classified Report).

responsivities derived from the wake scale to within a maximum difference of 20 percent of the stellar calibrations. The λ_e (4.2 μm) discrepancies are probably due to the red leak and the basic nature of the phenomenon. The physics of these events have been discussed in more detail by Murdock and Walker.[11]

The scaled inverse responsivities derived from the internal calibrators are given in column 11. Large scale geometry effects were anticipated due to the location of these sources on one side of the focal plane housing. These measurements were considered on the assumption that the internal scattering of the radiation within the focal plane housing would average these effects out. The internal consistencies of these pulses were also good, with typical deviations of 20 percent of the scaled mean value. These relative values are, for the most part, within 30 percent of those derived from the stars. Greater discrepancies exist for the λ_e (4.2 μm) again due, in part, to the red leak.

Once the calibrated inverse responsivities were derived, an in band irradiance or a magnitude was calculated for each observation by means of Eq. (1) or (6) respectively. The λ_e (4.2 μm) values were adjusted for the red leak by applying a correction term derived by assuming that the source had a blackbody distribution in this spectral region with a color temperature defined by the λ_e (11.0 μm) and λ_e (19.8 μm) observations. The correction term is accurate for temperatures greater than 400°K. Below this the λ_e (4.2 μm) measurements are very uncertain.

The calibration of the data from the last three flights were more difficult as each of these experiments used a different focal plane assembly and thus had to be calibrated individually. These experiments detected an insufficient number of reference stars on each detector to provide an adequate regression solution, so the reference list was augmented for each subsequent experiment with survey measurements in the mutually overlapping area from previous experiments. The calibration errors for these experiments were higher due to the larger uncertainties inherent in the previous survey measurements and the fewer total number of sources to calibrate against.

The small difference in wavelengths between the 11 μm and 20 μm shown in Table 1 were ignored in calibrating the southern hemisphere data. The λ_e (11.1 μm) and λ_e (19.6 μm) colors for the eighth experiment had a sufficient number of reference sources to calibrate each detector individually by the previously described technique.

The inverse responsivities for the λ_e (27.4) channels were derived by scaling the voltage responsivities measured at the Naval Electronics Laboratory Center (NELC)[12] for the focal plane assembly to the fluxes inferred from published data

12. Arrington, D.C., and Cisenman, W. L. (1973) Test Data for a 24-Element Array, 2600-15, NELC.

on GL2688, GL2495 = IRC + 30407, GL4114 = η Car and GL2390 = IRC + 10420 and a blackbody extrapolation to the asteroid Ceres based upon the color temperature defined by the λ_e (11.1 μm) and λ_e (19.6 μm) observations. The estimated calibration errors are between 30 and 50 percent.

The scaling factor obtained by this method agrees well with those derived from the λ_e (11.1 μm) and λ_e (19.6 μm) individual channels and is essentially the total system gain for each color. Unfortunately, these system gains were 4 to 4.5 times less than those calculated from the known optical gain[13] of the telescope and the electronic amplification as measured in the laboratory. If the amplifier gains are applied to the detector noise values measured at NELC, the result is within 50 percent of that observed during the flight.

The measured lower responsivity of the detectors was originally attributed to the illumination geometry effects observed by Sayre et al[4] for parallel biased detectors such as the ones used for the survey. However, Arrington et al[12, 14] noted that the detector responsivities decreased with increasing background flux. The NELC data[12, 14] indicated that, if account is made for the "blue" spectral leak in the λ_e (27.4 μm), the character of the responsivity decrease in each of the colors could be explained by a dilute 300°K background. This proved to be the case as an increase of the proper amount was observed in the detector response to the internal calibrators when the focal plane was optically sealed off from the rest of the sensor. This decrease in sensor sensivity unfortunately about compensated for the anticipated increase due to the sensor modifications performed for the southern hemisphere experiments.

After the calibrations were applied to the individual survey experiments, multiple observations on a single object obtained from the different flights were combined in a simple mean. Comparisons between the resulting final survey magnitudes and reference source magnitudes for all objects common to both lists are shown in Figures 3, 4, and 5. In Figure 3 the difference between the λ_e (4.2 μm) measured and reference magnitudes are plotted against the measured magnitudes. The vertical lines in this plot are the reported extreme on the reference sources. The same plot for the λ_e (11.0 μm) color is shown in Figure 4. Here the crosses are magnitudes taken from the work of Hall[15] who adopted a different set of reference values for many of the sources in common with the AFGL list. Finally, the same data for the λ_e (19.8 μm) is shown in Figure 5.

---

13. HI STAR II PROGRAM (1974) Final Report, Hughes Aircraft Company, Report No. p74-288 (Classified Report).

14. Arrington, D.C., and Eisenman, W.L. (1974) Test Data for a 24-Element Array, 2610-17, Naval Electronics Research Laboratories.

15. Hall, R.T. (1974) A Catalog of 10-μm Celestial Objects, SAMSO-TR-74-212.

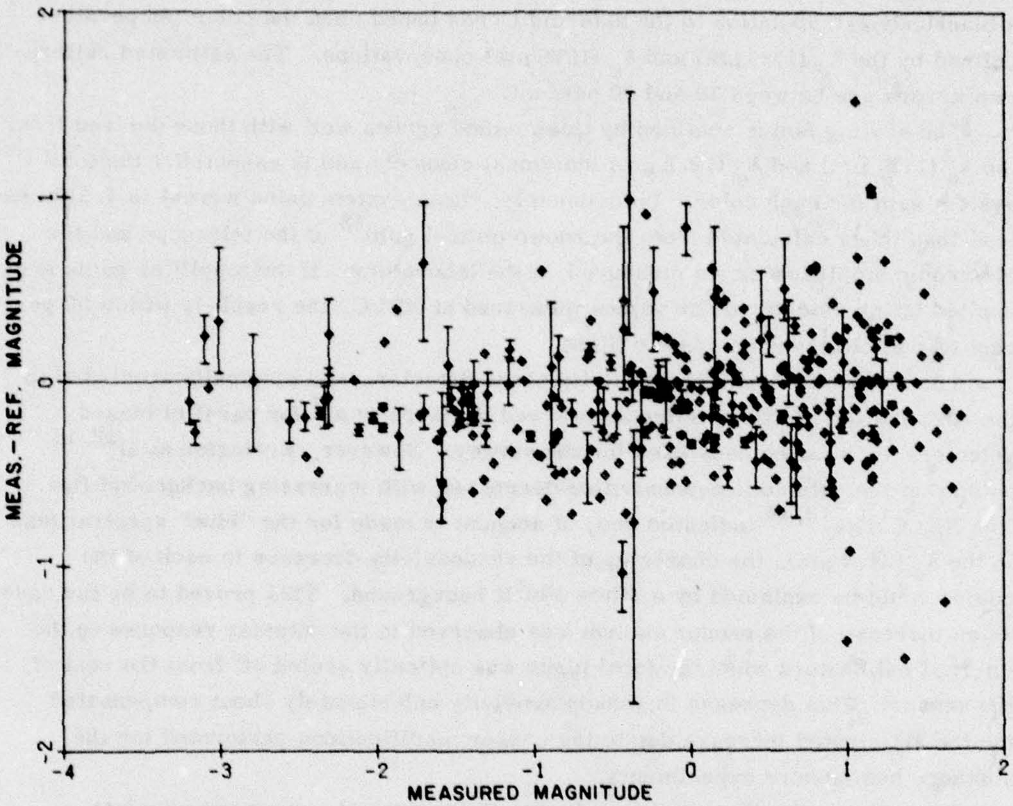

Figure 3. The Measured Minus Reference Star Magnitudes Plotted Against the Measured Magnitude at λ_e (4.2 μm) for all the Reference List Sources Observed During the AFGL Survey. *The vertical lines represent the range of values reported in the astronomical literature while the symbol bisected by the line is the adopted mean reference value for this source*

The AFGL survey is estimated to be statistically complete[1] down to magnitudes of m(4.2 μm) $\simeq$ +1.3, m(11.0 μm) $\simeq$ -1.1 and m(19.8 μm) $\simeq$ -3.1. Below these levels the measurement error is a significant factor in calculating the observed magnitudes. This is evident in Figures 3, 4, and 5 where the difference between the measured and reference magnitudes become rather large for measured magnitudes fainter than the aforementioned limits. Also it may be noted that at the fainter magnitudes there is a tendency for the measured quantities to be brighter than the reference values. This can be explained by the fact that at these levels a positive measurement error added to the true observed voltage of the source will yield a brighter than correct measurement while a negative error will cause the observation to fall below the detection threshold and, therefore, eliminate it from

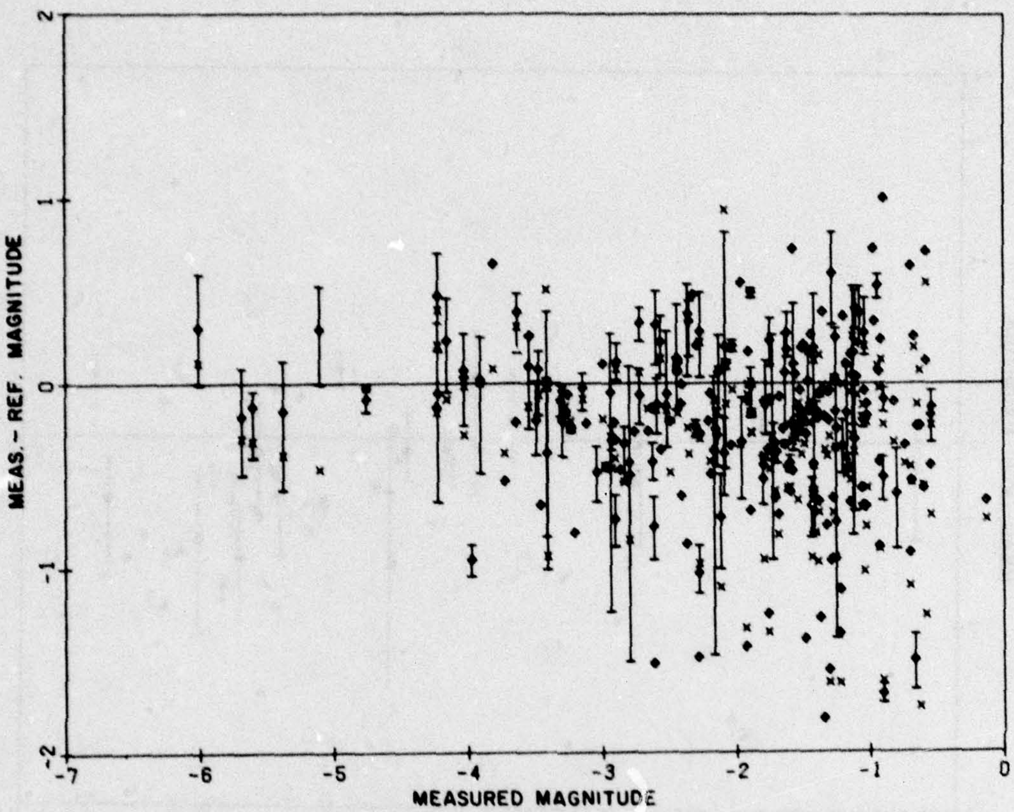

Figure 4. Comparison of the λ_e (11.0 μm) Measured Magnitudes and Their Respective Measured Minus Reference Magnitudes for all Reference List Sources Observed During the Survey. The points dotted with x's are reference magnitudes taken from the compilation of Hall.[15] Note that for most of the variable stars the value adopted by Hall[15] is different than that from the AFGL compilation. The other symbols have the same meaning as Figure 3

consideration. The threshold for a measurement to be included in the calibration was set to be equivalent to the limit of statistical completeness in each color, so this last effect should have been minimized in the calibration.

An indication of the accuracy of the calibration may be obtained from Table 3 which compares the observed magnitudes to the adopted standard magnitudes for 28 bright stars which are well measured in the infrared and are either known to be non-variable or have been used as infrared standard stars for various ground based photometric systems. As can be seen the two magnitudes agree within a few tenths of each other. For the stars in Table 3, the observed values in each color are, on the average, a tenth of a magnitude brighter than the standard magnitudes with root mean squared deviations of 0.2 magnitude about this mean difference.

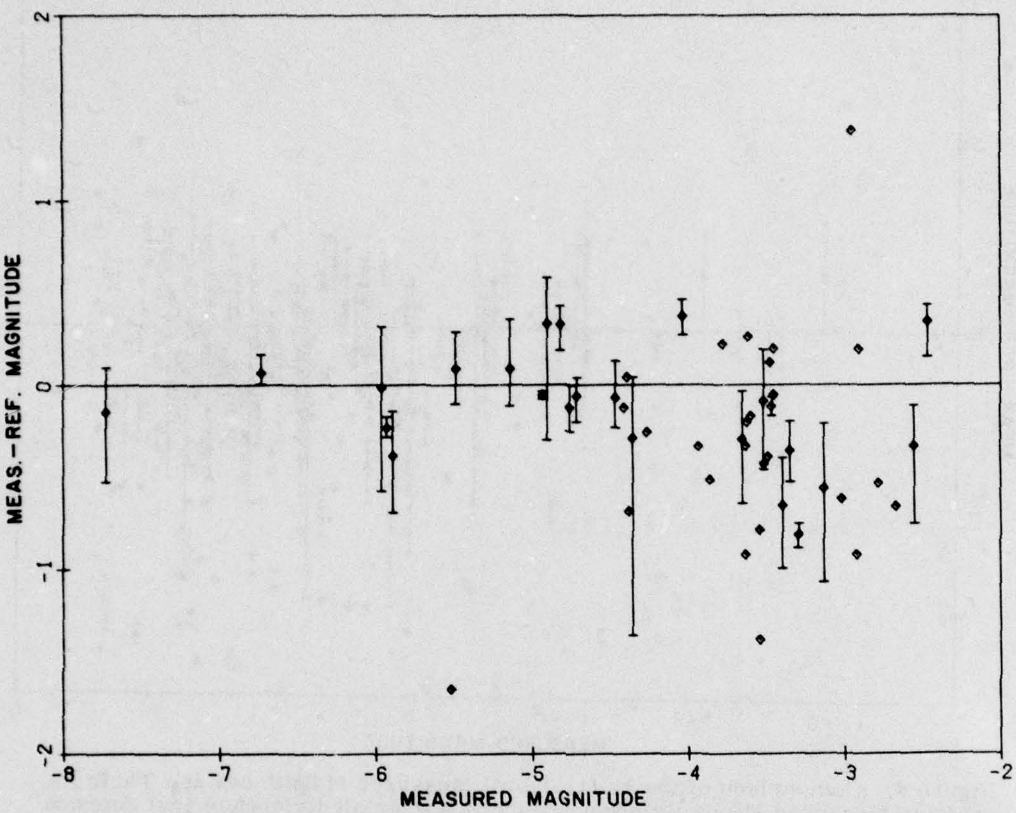

Figure 5. Comparison Between the Measured and Measured Minus Reference Magnitudes at λ_e (19.8 μm) for all Sources in Common With the AFGL Catalog[1] and the Reference List. Note the paucity of objects. The symbols have the same meaning as in Figure 3

Table 3. Observed and Reference Magnitudes for Stars Commonly Used as Infrared Standards

IRC	Name	m(4.2) obs	m(4.2) std	m(11.0) obs	m(11.0) std	m(19.8) obs	m(19.8) std
40019	β And	-2.0	-1.8	-2.3	-2.1		
00018	α Cet	-2.0	-1.7	-1.9	-1.9		
40054	ρ Per	-2.5	-2.1	-2.5	-2.3		
-10055	γ Eri	-1.3	-0.8	-1.6	-1.4		
20087	α Tau	-3.2	-2.9	-3.2	-3.0		
30100	ι Aur	-1.0	-0.6	-1.7	-1.0		
50139	α Aur	-2.1	-1.9	-2.3	-2.0		
10100	α Ori	-	-4.4	-5.6	-5.5	-5.9	-5.7
-20084	17 Lep	0.5	0.55	-1.5	-1.4		
20144	μ Gem	-2.2	-2.2	-2.2	-2.1		
-20105	α CMa	-1.2	-1.3	-1.4	-1.3		
30194	β Gem	-1.4	-1.2	-1.4	-1.3		
-10217	α Hya	-1.5	-1.4	-1.2	-1.3		
40218	μ VMa	-0.6	-0.8	-1.6	-1.2		
10235	56 Leo	-1.1	-0.8	-1.4	-1.2		
	γ Cru			-3.4	-3.4	-3.5	-3.4
00226	δ Vir	-1.5	-1.3	-1.5	-1.5		
20270	α Boo	-3.1	-3.0	-3.3	-3.1	-3.5	-3.1
-30228	σ Lib	-1.5	-1.4	-2.1	-1.4	-2.8	-2.3
-30265	α Sco			-4.9	-4.7	-4.9	-4.9
40283	30g Her	-2.4	-2.2	-2.8	-2.7		
10324	α Her			-4.0	-4.1	-4.4	-4.4
	89 Her	1.1	1.2	-1.3	-1.2		
50274	γ Dra	-1.6	-1.3	-1.8	-1.7		
40322	α Lyr	-0.4	0.0	-0.6	0.0		
-20558	υ Sgr	0.9	1.4	-1.1	-1.3		
10439	γ Aql	-0.8	-0.3	-1.1	-1.1		
60325	μ Cep	-2.4	-2.2	-4.0	-4.1	-4.7	-4.7
30504	β Peg	-2.5	-2.3	-2.6	-2.7		

4. CONCLUSIONS

Several significant observations may be made from the results of the calibration procedures used at AFGL for its space borne cryogenically cooled sensors:

(1) The linear slope over two orders in magnitude for each detector obtained from the least squares regression of the system magnitudes against the reference values for the combined data from the first six flights, attest not only to the linearity and stability of the system but demonstrate that stellar references are good calibration sources provided enough of them are observed.

(2) Primary standards, that is sources with precisely known spectral energy distributions, are not required. Spectral uncertainties and amplitude errors for small amplitude variable stars add in a random fashion such that the average calibration is correct. If enough stellar references are observed over an adequate dynamic range, the error in calculating the system responsivity is smaller than the error in the regression fit. Further, the standard deviation of the observed and reference magnitude is of the same size as the measured variation in responsivity over the surface of a detector.

(3) Rather surprisingly, a good calibration was obtained from a least squares fit of the square of the observed noise voltage to a known background irradiance. Although, this procedure suffers from lack of sensitivity and, for practical reasons restricts the dynamic range of the independent variable, it may have value in calibrating some of the spectral colors proposed for future systems where few, if any, reliable laboratory or celestial sources are known with any accuracy.

In conclusion, it was found that the stars provided excellent reference sources to calibrate space borne sensors if a sufficient number of them are observed to permit a meaningful regression solution.

References

1. Price, S.D., and Walker, R.G. (1976) The AFGL Four Color Sky Survey: Catalog of Observations at 4.2, 11.0, 19.8 and 27.4 μm, AFGL-TR-76-0205, Environmental Research Papers, No. 576.
2. Hickey, R.F. (1971) Performance Evaluation of the SAMSO/Hughes HI STAR Sensor, AEDC-TR-71-63 (Classified Report).
3. Nutt, K.W. (1973) Performance Evaluation of the HI STAR Sensor Using a New Integrating Sphere Target Source, AEDC-TR-73-142 (Classified Report).
4. Sayre, C., Arrington, D., Eisenman, W., and Merriam, J. (1976) Characteristics of Detectors Having Partially Illuminated Sensitive Areas, IRIS Meeting on Detectors.
5. Stromgren, B. (1937) Handbuch der Experimental Physik, ed. Wein and Hanms, Leipzig: Akademishe Verlags Gesellschaft M.B.H., 26:321.
6. Merrill, K.M. (1977) Infrared Observations of Late Type Stars, Invited Review Paper at I.A.V. Symposium No. 42.
7. Forrest, W.J., Gillett, F.C., and Stein, W.A. (1975) Circumstellar grain and the intrinsic polarization of starlight, Ap. J. 195:423.
8. Neugebauer, G., and Leighton, R.B. (1969) Two Micron Sky Survey, A Preliminary Catalog, NASA SP-3047.
9. Neugebauer, G. (1971) Unpublished extension to the IRC.
10. Hiatt, J. (1975) ARPA/Perkin-Elmer MARK VII Sensor Test, AEDC-TR-75-50 (Classified Report).
11. Murdock, T.L., and Walker, R.G. (1975) Infrared Signatures of High Altitude Reentry Wakes, AFCRL-TR-75-0083 (Classified Report).
12. Arrington, D.C., and Cisenman, W.L. (1973) Test Data for a 24-Element Array, 2600-15, NELC.
13. HI STAR II PROGRAM (1974) Final Report, Hughes Aircraft Company, Report No. p74-238 (Classified Report).

14. Arrington, D.C., and Eisenman, W.L. (1974) Test Data for a 24-Element Array, 2610-17, Naval Electronics Research Laboratories.

15. Hall, R.T. (1974) A Catalog of 10-μm Celestial Objects, SAMSO-TR-74-212.

Appendix A

The table in this appendix list the IRC source which comprised the reference star list used to calibrate the AFGL sensors. The first column lists the IRC number of the star while the second gives the star name, variable star or other designation. The maximum, mean and minimum magnitudes at λ_e (4.2 μm) adopted for this source is given in columns 3, 4 and 5, respectively. The respective λ_e (11.0 μm) values are listed in columns 6, 7 and 8 while columns 9, 10 and 11 give the λ_e (19.8 μm) magnitudes.

Note that in the name column, MUU and NUU were used to designate μ and ν in order to avoid possible confusion with variable star designations of MU and NU.

Table A1

IRC	NAME	4.2 MICRONS MAX	MEAN	MIN	11 MICRONS MAX	MEAN	MIN	19.8 MICRONS MAX	MEAN	MIN
13	3 PSC	1.51	1.51	1.51	.22	.22	.22			
30	OMI CET	-3.56	-3.66	-3.66	-5.10	-5.40	-5.63	-5.39	-5.82	-6.01
39	ALF CET	-1.70	-1.72	-1.74	-1.70	-1.87	-1.97	-1.68	-2.05	-2.30
47	10 TAU	2.91	2.91	2.91						
56	W ORI	-.51	-.51	-.51	-1.70	-1.72	-1.74	-1.97	-1.97	-1.97
74	S ORI	-.79	-.79	-.79	-1.60	-1.60	-1.60			
75	DEL ORI	2.89	2.89	2.89						
79	EPS ORI	2.14	2.14	2.14						
81	ZET ORI	2.33	2.33	2.33						
150	IOT HYA	.68	.68	.68						
217	SS VIR	.32	.32	.32	-.99	-.99	-.99			
221	BS 4917	.62	.62	.62						
223	GAM VIR	1.78	1.78	1.78						
224	RU VIR	-.33	-.33	-.33	-1.84	-1.98	-2.10			
226	DEL VIR	-1.23	-1.27	-1.31	-1.29	-1.47	-1.63	-2.05	-2.05	-2.05
230	SW VIR	-1.85	-1.89	-1.89	-3.10	-3.12	-3.13	-4.01	-4.01	-4.01
243	RS VIR	.55	.55	.55	-1.26	-1.26	-1.26			
266	3747	1.72	1.72	1.72	-1.54	-1.54	-1.54			
280	DEL OPH	-1.43	-1.43	-1.43	-.51	-.51	-.51	-1.77	-1.77	-1.77
282	EPS OPH	.93	.93	.93						
304	SIG OPH	.86	.86	.86						
317	BET OPH	.08	.05	.08	1.00	1.00	1.00			
363	5093	.73	.73	.73	-2.40	-2.40	-2.40			
365	2176	-.54	-.54	-.54	-2.80	-2.80	-2.80			
377	AR AQL	2.52	2.52	2.52	1.90	1.90	1.90			
389		.48	.44	.48	-1.14	-1.28	-1.40			
395	UW AQL	1.46	1.45	1.46						
439	V374 AQL	.55	.53	.53	.13	-.50	-.90			
458	SR AQL	-.97	-.97	-.97	-2.40	-2.40	-2.40			
490		.04	.04	.04	-1.20	-1.20	-1.20			
499	RV AQR				-2.50	-2.50	-2.50			
507	BD-2-5597				.80	.80	.80			
509	GC 30492				-2.90	-2.90	-2.90			
513	ALF AQR	.95	.95	.95	.90	.90	.90			
517	35 PSC	2.16	2.16	2.16						
532	TX PSC	-.85	-.85	-.85	-1.26	-1.32	-1.37			
10011	CIT 3	-.65	-1.39	-1.96	-2.58	-3.42	-3.80	-4.61	-5.24	-5.49
10059	NML TAU	-1.93	-2.35	-2.69	-3.58	-4.17	-4.55	-5.39	-5.58	-5.76
10084	GAM ORI	2.35	2.35	2.35	-1.45	-1.45	-1.45			
10102	ALF ORI	-4.29	-4.35	-4.42	-5.20	-5.48	-5.56	-5.65	-5.70	-5.76
10116		1.82	1.82	1.82						
10119	BN MON	1.67	1.67	1.67						
10121	BL ORI	.46	.46	.46	-.16	-.16	-.16			
10146	SV MON	1.08	1.09	1.08	-.27	-.27	-.27			
10154	R CMI	1.97	1.97	1.97	.97	.97	.97			
10162	ZZ CMI				1.12	1.12	1.12	1.37	1.37	1.37
10170	ALF CMI	-.69	-.69	-.69	-.86	-.86	-.86	-1.13	-1.13	-1.13
10171	U CMI	2.17	2.17	2.17	.78	.78	.78			
10185	R CNC	-1.09	-1.23	-1.35	-2.50	-2.54	-2.56	-2.82	-2.99	-3.15
10186	BET CNC	-.07	-.47	-.37	.51	.51	.51			
10189	27 CNC	.20	.20	.20						
10196	ZET HYA	.59	.59	.59						
10199	ST CNC	-.01	-.01	-.01	-.91	-.91	-.91			
10215	R LEO	-3.20	-3.35	-3.46	-4.40	-4.70	-4.93	-5.03	-5.23	-5.50
10216		-3.52	-4.14	-4.42	-7.34	-7.47	-7.70	-7.50	-8.63	-9.40

Table A1 (Cont.)

IRC	NAME	4.2 MICRONS MAX	MEAN	MIN	11 MICRONS MAX	MEAN	MIN	19.8 MICRONS MAX	MEAN	MIN
10224	RI LEO	.52	.44	.37	.27	.22	.18	3.63	3.63	3.63
10226	ALF LEO	1.56	1.55	1.55	1.30	.45	-.04	1.78	1.78	1.78
10234	W LEO				-.26	-.39	-.50			
10235	VY LEO	-.77	-.77	-.77	-1.24	-1.24	-1.24			
10236	SC 15361	1.14	1.14	1.14	-.30	-.30	-.30			
10237	73 LEO	1.31	1.31	1.31	1.01	1.41	1.01			
10243	OME VIR	-.13	-.13	-.13	-.57	-.57	-.57			
10245	NUU VIR	-.11	-.11	-.11						
10256	R VIR	.10	.10	.10	.64	.64	.64			
10261	EPS VIR	.73	.73	.73						
10262	RT VIR							-3.42	-3.42	-3.42
10290	S SER	.51	.51	.51	-.71	-.86	-1.00			
10294	ALF SER	.03	.03	.03	.51	.51	.51			
10295	LAM SER	3.00	2.98	2.96						
10307	29 HER	1.02	1.02	1.02						
10315	KAP OPH	.52	.52	.52						
10318	RS 6737	.40	.40	.40						
10322		-.11	-.20	-.29	-1.66	-1.84	-2.00			
10324	ALF HER	-3.58	-3.58	-3.58	-4.06	-4.06	-4.06	-4.44	-4.44	-4.44
10352	V454 OPH				-1.80	-1.80	-1.80			
10365	V111 OPH	-.39	-.87	-1.27	-2.40	-3.03	-3.40			
10366	X OPH	-1.47	-1.47	-1.47	-2.30	-2.55	-2.76	-3.10	-3.10	-3.10
10374					-1.50	-1.50	-1.50			
10384	V913 AQL	.52	.52	.52						
10391	V492 AQL	1.33	1.33	1.33						
10392	EPS AQL	1.43	1.43	1.43						
10401		-.19	-.19	-.19	-2.50	-2.50	-2.50			
10405	R AQL	-1.22	-1.37	-1.50	-2.30	-2.58	-2.87	-3.30	-3.35	-3.40
10407	V844 AQL	.19	.19	.19						
10409	BD-13-4919	1.44	1.44	1.44	.50	.50	.50			
10420	5752	-.20	-.36	-.50	-4.20	-4.36	-4.50	-6.50	-6.50	-6.50
10430	MUU AQL	1.57	1.57	1.57						
10439	GAM AQL	-.32	-.32	-.32	-1.13	-1.13	-1.13	-1.12	-1.12	-1.12
10441	ALF AQL	.19	.19	.19	.26	.26	.26			
10444	BET AQL	1.55	1.55	1.55						
10474	THE DEL	2.12	2.12	2.12						
10499	UU PEG				-2.80	-2.80	-2.80			
10503	EPS PEG				-2.30	-2.30	-2.30	-1.20	-1.20	-1.20
10510					-1.50	-1.50	-1.50			
10514	RS PEG				-1.20	-1.20	-1.20			
10523					-1.40	-1.40	-1.40			
10526	ALF PEG	2.36	2.36	2.36	2.18	2.18	2.18			
10527	R PEG	-.46	-.46	-.46	-.60	-1.61	-1.90	-2.30	-2.30	-2.30
20004	CHI PEG	.38	.38	.38						
20007	TV PSC	-.47	-.47	-.47						
20013	ZET AND	3.62	3.62	3.62						
20038	ALF ARI	-.69	-.63	-.59	-.77	-.79	-.80	-1.24	-1.24	-1.24
20051	R7 ARI	-1.33	-1.33	-1.33						
20063	ETA TAU	2.87	2.87	2.87						
20076	DEL TAU	1.01	1.01	1.01	-.40	-.40	-.40			
20087	ALF TAU	-2.82	-2.89	-2.95	-2.97	-2.99	-3.00	-3.00	-3.02	-3.04
20112	119 TAU	-1.04	-1.15	-1.30	-1.26	-1.30	-1.35			
20113	ZET TAU	2.51	2.51	2.51						
20121	Y TAU	-.38	-.38	-.38	-1.90	-1.92	-1.93	-1.78	-1.78	-1.78
20125	CHI1 ORI	2.69	2.69	2.69						

Table A1 (Cont.)

IRC	NAME	4.2 MICRONS MAX	MEAN	MIN	11 MICRONS MAX	MEAN	MIN	19.8 MICRONS MAX	MEAN	MIN
20127	U OPI	-1.05	-1.32	-1.53	-2.82	-2.91	-3.00			
20134	TV GEM	.51	.51	.51	-1.27	-1.27	-1.27			
20135	WY GEM	1.72	1.58	1.46	1.46	1.21	1.00			
20136	BU GEM	.75	.75	.75	-.98	-.98	-.98			
20139	ETA GEM	-1.34	-1.44	-1.53	-1.74	-1.75	-1.76			
20144	MUU GEM	-2.16	-2.16	-2.16	-2.14	-2.14	-2.14	-2.32	-2.32	-2.32
20146	SX GEM	-1.43	-1.43	-1.43						
20154	CAM GEM				2.19	2.19	2.19			
20163	41 GEM	1.70	1.70	1.70						
20169	ZET GEM	2.10	2.10	2.10	2.20	2.20	2.20			
20171	R GEM	1.60	1.60	1.60	.58	.58	.58			
20197	VV CNC	-.47	-.47	-.47	1.02	-2.12	-2.84	.36	.36	.36
20200	THE CNC	.59	.59	.59						
20206	X CNC	-.04	-.04	-.04	-.92	-.92	-.92			
20207	T CNC	.51	.51	.51	-.65	-.65	-.65			
20211	LAM LEO	.41	.41	.41						
20219	GAM1 LEO	-.79	-.79	-.79	-1.15	-1.15	-1.15	-1.24	-1.24	-1.24
20227	72 LEO	-.11	-.11	-.11	-.38	-.38	-.38			
20251	36 COM	.60	.60	.60						
20254	40 COM	-.22	-.22	-.22	-.62	-.62	-.62			
20257		1.54	1.54	1.54	1.10	1.10	1.10			
20263	UPS BOO	.18	.18	.18						
20267	ETA BOO	1.28	1.28	1.28	-2.67	-2.67	-2.67			
20270	ALF BOO	-3.04	-3.04	-3.04	-2.90	-3.09	-3.25	-3.10	-3.10	-3.10
20276	XI BOO	2.45	2.45	2.45						
20281	WX SER	1.30	1.07	.87	.90	-1.08	-1.70	-1.80	-2.22	-2.44
20282	TAU4 SER	-1.17	-1.17	-1.17	-2.08	-2.08	-2.08			
20284	KAP SER	-.19	-.19	-.19						
20285	R SER	.07	.07	.07	-1.16	-1.16	-1.16			
20288	CS 5924	1.23	1.23	1.23						
20296	GAM HER	2.78	2.78	2.78						
20298	U HER	-.96	-1.02	-1.07	-2.30	-2.51	-2.60	-2.40	-2.74	-3.00
20326	16032				-2.50	-2.66	-2.80			
20329	MW HER	.74	.42	.18	-2.35	-2.38	-2.40	-4.33	-4.33	-4.33
20364	109 HER	.96	.96	.96						
20370		-.70	-2.81	-3.85	-1.49	-2.91	-3.50			
20392	HT 4-2	1.64	1.64	1.64						
20417	HT 4-1	2.19	2.19	2.19						
20419	HC 61	3.48	3.48	3.48						
20426	ALF SGE	2.46	2.46	2.46						
20427	BET SGE	1.94	1.94	1.94						
20433	DEL SGE	-1.07	-1.07	-1.07						
20438		.71	.71	.71						
20439	BD+22-3840	-.74	-.98	-1.09	-1.69	-1.86	-2.00			
20445	GAM SGE	-.45	-.45	-.45						
20481	U DEL	-.57	-.57	-.57	-1.74	-1.74	-1.74			
20505	1 PEG	1.40	1.40	1.40						
20526	GC 30777				-.70	-.70	-.70			
20539	BS 8714				-.30	-.30	-.30			
20557	PSI PEG	-.31	-.31	-.31						
30004	ALF AND				2.46	2.46	2.46	1.46	1.46	1.46
30014	DEL AND	-.05	-.05	-.05	-.01	-.01	-.01			
30021		1.07	1.05	1.03	-1.60	-1.88	-2.10			
30044	R TRI							-1.00	-1.00	-1.00
30058	BS 991	1.32	1.32	1.32						

Table A1 (Cont.)

IRC	NAME	4.2 MICRONS MAX	4.2 MICRONS MEAN	4.2 MICRONS MIN	11 MICRONS MAX	11 MICRONS MEAN	11 MICRONS MIN	19.8 MICRONS MAX	19.8 MICRONS MEAN	19.8 MICRONS MIN
30068	ZET PER	2.66	2.66	2.66						
30073	BS 1286	2.36	2.36	2.36						
30100	IOT AUR	-.58	-.58	-.58	-.97	-.97	-.97			
30114	S AUR				-1.30	-1.30	-1.30			
30124	BS 1933	.50	.50	.50						
30129	BS 2018	.99	.99	.99						
30138		2.37	2.37	2.37						
30143	TU GEM	.21	.21	.21	-.99	-.99	-.99			
30188	ALF GEM	1.38	1.39	1.38	1.44	1.44	1.44			
30194	BET GEM	-1.16	-1.21	-1.26	-1.30	-1.32	-1.33	-1.24	-1.27	-1.30
30204	RHO2 CNC	-.07	-.07	-.07						
30209	BS CNC	-1.82	-1.83	-1.85	-2.95	-3.05	-3.13	-3.60	-3.60	-3.60
30210	ALF LYN	-.80	-.80	-.80						
30215	R LMI	-1.05	-1.26	-1.39	-2.50	-2.75	-2.83	-3.44	-3.44	-3.44
30219	RW LMI	-1.79	-2.73	-3.01	-4.20	-4.97	-5.40	-5.06	-5.13	-5.20
30220		1.25	1.29	1.29	-.17	-.17	-.17			
30230	NUU UMA	.09	.09	.09						
30246	BET COM	2.72	2.72	2.72						
30251	BS 5219	-.24	-.24	-.24						
30257	RX BOO	-2.09	-2.24	-2.32	-3.30	-3.55	-3.65	-4.29	-4.29	-4.29
30259	RHO BOO	.48	.48	.48						
30260	R BOO	1.17	1.17	1.17	.42	.25	.10			
30261	RV BOO	-.30	-.30	-.30	-1.56	-1.56	-1.56			
30262	RW BOO	.36	.34	.32	-.81	-.89	-.96			
30263	W BOO	.24	.23	.22	-.07	-.15	-.22			
30271	DEL BOO	.88	.88	.88						
30272	S CRB	-.81	-.90	-.98	-2.83	-2.99	-3.12	-2.94	-3.30	-3.50
30280	EPS CRB	1.05	1.05	1.05						
30283	RU HER	0.00	-.23	-.38	-.77	-1.37	-1.99	-1.89	-1.89	-1.89
30292		1.47	1.31	1.17	-.80	-.83	-.85			
30294	ZET HER	1.06	1.06	1.06						
30343	BET LYR	2.20	2.20	2.20	-.06	-.06	-.06			
30370	BET CYG	-.09	-.09	-.09						
30374		.30	.30	.30	-2.30	-2.30	-2.30			
30382	TT CYG	1.43	1.43	1.43	.80	.80	.80			
30391		1.54	1.54	1.54						
30395	CHI CYG	-2.42	-2.80	-3.05	-3.42	-3.93	-4.16	-4.24	-4.40	-4.60
30401	ETA CYG	1.48	1.49	1.48						
30407	HFE 63	2.08	2.08	2.08	-.10	-.10	-.10			
30412		1.17	1.17	1.17						
30448	30 VUL	2.03	2.03	2.03						
30450	52 CYG	1.57	1.57	1.57						
30451	EPS CYG	-.05	-.05	-.05						
30464	UX CYG	1.07	1.07	1.07	-.50	-.50	-.50			
30472	ZET CYG	.93	.93	.93						
30481	TH PEG				-2.20	-2.23	-2.26	-3.05	-3.05	-3.05
30485	IOT PEG	2.59	2.59	2.59						
30499	ETA PEG				.50	.50	.50	.54	.54	.54
30504	BET PEG	-2.20	-2.27	-2.35	-2.32	-2.48	-2.62	-2.17	-2.41	-2.60
30509					-2.00	-2.00	-2.00			
30522	Z PEG	.92	.92	.92						
40004		.02	.02	.02	-2.40	-2.40	-2.40			
40006	VX AND	.41	.41	.41						
40009	R AND	-.43	-.97	-1.32	-2.60	-2.60	-2.60	-3.06	-3.43	-3.71
40011	AQ AND	1.18	1.19	1.18	.25	.25	.25			

Table A1 (Cont.)

		4.2 MICRONS			11 MICRONS			19.8 MICRONS		
IRC	NAME	MAX	MEAN	MIN	MAX	MEAN	MIN	MAX	MEAN	MIN
40014					2.29	2.29	2.29	1.85	1.85	1.85
40019	BET AND	-1.81	-1.83	-1.86	-2.01	-2.07	-2.10	-1.93	-2.11	-2.26
40024	UPS AND	2.76	2.76	2.76						
40034	GAM1 AND	-.84	-.84	-.84						
40037	W AND				-1.70	-1.70	-1.70			
40054	RHO PER	-2.05	-2.05	-2.05	-2.28	-2.29	-2.30	-2.37	-2.44	-2.50
40068	MUU PER	-.04	-.04	-.04	-.20	-.20	-.20			
40091	LK HALP111	-.23	-.23	-.23	-2.40	-2.40	-2.40	-3.70	-3.70	-3.70
40093	58 PER	1.09	1.09	1.09						
40105		1.90	1.90	1.90						
40109	EPS AUR	.94	.94	.94	1.05	1.05	1.05			
40148	BET AUR	1.86	1.86	1.86						
40156	12285	.79	.79	.79	-1.30	-1.30	-1.30			
40158	UU AUR	-.79	-.79	-.79	-2.15	-2.18	-2.20	-2.18	-2.18	-2.18
40195	31 LYN	.30	.30	.30						
40211	BS 3579	2.85	2.85	2.85						
40218	MUU UMA	-.78	-.81	-.85	-1.11	-1.16	-1.20			
40224	PSI UMA	.26	.26	.26						
40238	U CVN	1.68	1.69	1.68	.35	.35	.35			
40248	R CVN	-.07	-.07	-.07	-1.29	-1.29	-1.29			
40253	BS 5299	-.46	-.46	-.46	-.38	-.38	-.38			
40271	RR CRB	.88	.88	.88	.44	.44	.44			
40273	V CRB	.96	.96	.96	-.85	-.85	-.85			
40275	2 HER	.46	.46	.46				-3.55	-3.55	-3.55
40278	TAU CRB	2.02	2.02	2.02						
40283	G HER	-2.12	-2.23	-2.33	-2.66	-2.72	-2.79	-2.80	-2.90	-3.00
40287	ETA HER	1.20	1.20	1.20						
40293	UM HER	1.20	1.20	1.20	-.70	-.70	-.70			
40321	T LYR	-.19	-.29	-.38	-.30	-1.10	-1.55	-1.35	-1.35	-1.35
40322	ALF LYR	-.01	-.01	-.01	-.03	-.03	-.03	-.08	-.08	-.08
40323	XY LYR	-.35	-.49	-.61	-.69	-1.01	-1.26			
40331	DEL2 LYR	-1.25	-1.25	-1.25	-1.66	-1.66	-1.66			
40334	R LYR	-2.08	-2.23	-2.39	-2.17	-2.46	-2.80	-2.62	-2.81	-2.90
40341	THE LYR	1.45	1.45	1.45						
40360	AA CYG	.46	.46	.46						
40397	RS CYG	1.26	1.26	1.26	.52	.52	.52			
40406	35 4077	.88	.88	.88						
40408	RI CYG	-.03	-.03	-.03	-2.40	-2.74	-2.90	-3.65	-3.65	-3.65
40409	RC CYG	-.20	-.22	-.25	-1.70	-2.89	-3.21	-3.87	-3.87	-3.87
40411	GAM CYG	.70	.67	.65	.80	.67	.56			
40415	KY CYG	-.71	-.71	-.71	-2.50	-2.50	-2.50			
40418	V441 CYG	1.32	1.32	1.32						
40424	RW CYG	.11	.05	-.01	-2.50	-2.69	-2.80	-3.43	-3.43	-3.43
40427	MWC 349				-1.73	-1.73	-1.73	-2.71	-2.71	-2.71
40431	HC 2	.45	.39	.32	-1.80	-1.80	-1.80			
40432	CIT 10	1.25	.87	.59	1.00	.84	.70			
40434	HC 1	.30	.27	.24	-1.70	-1.70	-1.70			
40440	HC 6	2.00	2.00	2.00						
40441	V446 CYG				-1.30	-1.30	-1.30			
40442	DG CYG	.59	.59	.59	-.80	-.80	-.80			
40445	CIT 13	-.88	-.88	-.88	-1.88	-1.88	-1.88			
40448	NML CYG	-2.35	-2.57	-2.76	-5.19	-5.51	-5.77	-6.74	-6.80	-6.90
40464	BS 8062	.59	.59	.59						
40468	XI CYG	.01	-.02	-.04	-.07	-.14	-.20	-.18	-.18	-.18
40469	61 CYG	1.69	1.58	1.49						

Table A1 (Cont.)

		4.2 MICRONS			11 MICRONS			19.8 MICRONS		
IRC	NAME	MAX	MEAN	MIN	MAX	MEAN	MIN	MAX	MEAN	MIN
40483		.75	.69	.64	-1.20	-1.67	-2.00			
40489	V460 CYG	1.34	.41	-.10	.79	-.37	-1.04			
40491	9V CYG	.12	.12	.12	-1.11	-1.11	-1.11			
40512	S LAC	1.78	1.78	1.78	1.05	1.05	1.05			
40540		-1.20	-1.20	-1.20	-3.80	-3.80	-3.80			
40545		1.14	1.14	1.14						
50039		.17	.17	.17						
50043	BD+44-398	-1.35	-1.35	-1.35						
50052	XX PER	.73	.73	.73						
50072	THE PER	2.94	2.94	2.94						
50086	IOT PER	2.65	2.65	2.65						
50089	1.34	1.14	1.14	1.14						
50095	ALF PER	.53	.49	.44	.46	.30	.16	.58	.58	.58
50096	CIT 5	-1.55	-1.55	-1.55	-3.13	-3.22	-3.30	-3.35	-3.35	-3.35
50111	MUU PER	1.78	1.78	1.78						
50137		.26	.03	-.18	-1.62	-2.28	-2.90	-4.00	-4.00	-4.00
50139	ALF AUR	-1.83	-1.86	-1.99	-2.00	-2.00	-2.01	-1.98	-2.02	-2.05
50156	PI AUR	-1.19	-1.19	-1.19						
50164	PSI1 AUR	.05	.05	.05	.13	.13	.13			
50180	Y LYN	-.52	-.59	-.66	-1.40	-1.69	-1.90			
50213	CHI UMA	.70	.70	.70						
50215	GAM UMA	2.56	2.56	2.56						
50219	Y CVN	-1.22	-1.31	-1.39	-1.95	-2.19	-2.39			
50222	TU CVN	-.37	-.37	-.37	-.50	-.50	-.50			
50226	V CVN	.91	.75	.70	-1.40	-1.47	-1.53			
50231	83 UMA	.14	.14	.14	.69	.69	.69			
50233	ETA UMA	1.31	1.31	1.31						
50246	SI HER	-.72	-.72	-.72	-1.70	-1.70	-1.70			
50248	X HER	-1.51	-1.55	-1.59	-2.95	-3.06	-3.18	-3.74	-3.74	-3.74
50273	OP HER	.14	-.09	-.28	-.74	-.74	-.74			
50274	GAM DRA	-1.29	-1.30	-1.30	-1.50	-1.66	-1.90			
50291	KAP CYG	1.64	1.64	1.64						
50294	CH CYG	-1.31	-1.34	-1.36	-2.57	-2.62	-2.70	-3.09	-3.09	-3.09
50301	P CYG	.19	.19	.19	-.90	-1.17	-1.30	-2.00	-2.00	-2.00
50308	DEL CYG	2.65	2.65	2.65						
50316	SV CYG	.91	.91	.91						
50324	U CYG	.43	.10	-.15	-1.40	-1.51	-1.61			
50337	ALF CYG	.80	.77	.74	.83	.78	.73	-.02	-.02	-.02
50338	V CYG	-1.39	-1.57	-1.72	-3.30	-3.64	-3.80	-3.88	-3.88	-3.88
50347	97 CYG	.20	.20	.20	-1.30	-1.30	-1.30			
50351	AZ CYG	.71	.71	.71	-1.70	-1.70	-1.70	-2.76	-2.76	-2.76
50357		-.59	-.59	-.59	-1.76	-1.89	-2.00			
50362		1.13	1.13	1.13						
50385	RHO CYG	1.84	1.84	1.84						
50409	LW CYG	.69	.69	.69						
50417	PS 8421	.67	.67	.67						
50446	U LAC	.40	.35	.32	-1.00	-1.00	-1.00			
50452	PS 8726	.50	.50	.50						
50484	R CAS	-2.23	-2.35	-2.46	-4.10	-4.10	-4.10	-5.01	-5.15	-5.25
60001	Y CAS	.10	.10	.10						
60004	BET CAS	1.33	1.33	1.33	1.02	1.02	1.02	1.34	1.34	1.34
60005	BD+63-3	1.01	1.01	1.01						
60009	T CAS	-1.45	-1.54	-1.63	-2.61	-2.79	-2.93	-3.45	-3.45	-3.45
60017	ALF CAS	-.02	-.02	-.02	-.41	-.41	-.41			
60019	ETA CAS	1.87	1.87	1.87	1.94	1.94	1.94			

Table A1 (Cont.)

IRC	NAME	4.2 MICRONS MAX	4.2 MICRONS MEAN	4.2 MICRONS MIN	11 MICRONS MAX	11 MICRONS MEAN	11 MICRONS MIN	19.8 MICRONS MAX	19.8 MICRONS MEAN	19.8 MICRONS MIN
60020	1,23	2.33	2.33	2.33						
60031	GAM CAS	2.88	2.88	2.88	.80	.80	.80			
60039	HS CAS	1.85	1.85	1.85						
60040	BD+61-219	2.11	2.11	2.11						
60046	PHI CAS	1.71	1.71	1.71	1.88	1.88	1.88			
60061		2.39	2.39	2.39						
60074	KK PER	1.58	1.58	1.58						
60078	BU PER	1.63	1.63	1.63						
60079	T PER	2.05	2.05	2.05						
60081	HD 14242	2.00	2.00	2.00						
60082	AD PER	1.85	1.71	1.58	.55	.55	.55			
60083	FZ PER	2.74	2.30	1.98	1.00	1.00	1.00			
60085	HD 14404	2.01	2.01	2.01						
60086	SU PER	1.35	1.15	.37	-.36	-.36	-.36			
60087	RS PER	.99	.99	.99						
60088	S PER	.26	.18	.10	-1.29	-2.37	-2.89	-3.01	-3.36	-3.62
60089	HD 14580	2.57	2.57	2.57						
60090	HD 14826	1.41	1.41	1.41						
60091		1.11	1.11	1.11	.47	.47	.47			
60092		-.23	-.23	-.23	-2.50	-2.50	-2.50			
60093	YZ PER	1.68	1.54	1.42	-.25	-.25	-.25			
60094	GP CAS	1.30	1.30	1.30						
60097	W PER	1.24	1.24	1.24	-1.25	-1.28	-1.30	-2.41	-2.48	-2.54
60098	ETA PER	-.19	-.19	-.19						
60100		1.34	1.34	1.34						
60106	1,31	1.58	1.58	1.58						
60110	TO PER	.22	.22	.22						
60111		1.40	1.40	1.40						
60117	BS 1009	.16	.16	.16						
60120	BS 1040	2.72	2.72	2.72						
60124	U CAM	.05	.05	.05						
60125	BS 1105	-.10	-.10	-.10						
60126	BS 1112	1.37	1.37	1.37						
60139		2.22	2.22	2.22						
60144		.37	.37	.37						
60150	TX CAM	.22	.22	.22	-1.00	-3.43	-4.12	-4.50	-4.50	-4.50
60179	R LYN	1.02	1.02	1.02	.04	.04	.04			
60208	ALF UMA	-.70	-.73	-.75	-.81	-.85	-.88	-.81	-.81	-.81
60213	Z UMA	.15	.13	.10	-.74	-.81	-.87			
60215	RY UMA	2.33	2.27	2.21	.41	.29	.19			
60233	ICT DRA	.47	.47	.47						
60242	ETA DRA	.37	.37	.37						
60251	TY DRA				-1.70	-1.70	-1.70			
60255	T DRA	.81	.60	.43	-.69	-1.80	-2.20	-2.01	-2.01	-2.01
60296	UU CEP	2.09	2.09	2.09						
60298	ETA CEP	1.15	1.15	1.15						
60310	ALF CEP	1.80	1.80	1.80						
60313	BGC 5481	.36	.25	.15						
60317	SW CEP	1.10	1.10	1.10						
60325	MUU CEP	-2.17	-2.20	-2.23	-3.80	-4.10	-4.30	-4.52	-4.66	-4.76
60326	NUU CEP	2.63	2.63	2.63						
60333	VV CEP	-.24	-.39	-.52	-.72	-.72	-.72			
60334	HT 1-1	.61	.61	.61						
60336	HT 1-3	1.36	1.35	1.36						
60343	AZ CEP	1.82	1.82	1.92						

Table A1 (Cont.)

IRC	NAME	4.2 MICRONS MAX	MEAN	MIN	11 MICRONS MAX	MEAN	MIN	19.8 MICRONS MAX	MEAN	MIN
60344	ZET CEP	.16	.05	-.05	-.10	-.10	-.10			
60353	EW CEP	1.46	1.45	1.45	-1.20	-1.24	-1.30	-2.16	-2.16	-2.16
60356	DEL CEP	2.30	2.30	2.30	2.20	2.20	2.20			
60357	ST CEP	1.54	1.54	1.54	-1.00	-1.00	-1.00			
60361	2,25	1.02	1.02	1.02						
60362	W CEP	1.39	1.24	1.11	-1.70	-1.70	-1.70	-2.49	-2.49	-2.49
60367	2,78	1.88	1.88	1.88						
60374	2,79	.95	.95	.95						
60377		1.91	1.91	1.91						
60379	RS 8752	1.41	1.14	.87	1.62	.70	.43			
60389	V CAS	-.06	-.06	-.06	-1.33	-1.33	-1.33			
60410	V35A CAS	1.10	1.10	1.10						
60416	BS 8999	1.17	1.17	1.17						
60417	PZ CAS	.09	.09	.08	-2.70	-2.92	-3.10			
60429	TZ CAS	1.55	1.55	1.55	-1.20	-1.20	-1.20			
60428	RHO CAS	2.83	2.83	2.83	2.43	2.43	2.43			
60433	W7 CAS	.50	.32	.17	-.04	-.04	-.04			
70003		.92	.92	.92						
70016	SD+74-46				-.10	-.10	-.10			
70026	S CAS				-1.10	-1.10	-1.10			
70046	BS 1155				-.55	-.55	-.55			
70066		-.26	-.26	-.26	-2.02	-2.17	-2.30			
70067	V CAM	.39	.39	.39						
70097	RHO UMA	-.48	-.48	-.48	-.40	-.40	-.40	-2.20	-2.20	-2.20
70100	VY UMA	.28	-.31	-.69	-.39	-.39	-.39			
70107	LAM DRA	-.39	-.39	-.39	.38	.38	.38			
70116	RY DRA	-.59	-.59	-.59	-1.19	-1.31	-1.50			
70124	U UMI	.50	.49	.48	-.60	-.77	-.92			
70126	RR UMI	-.79	-.79	-.79	-1.08	-1.08	-1.08			
70136	R DRA	1.81	1.81	1.81	.44	.44	.44			
70150	DEL DRA	.76	.76	.76						
70158	SIG DRA	2.52	2.46	2.41						
70160	EPS DRA	1.56	1.56	1.56						
70168	T CEP	-2.17	-2.17	-2.17	-3.00	-3.12	-3.20	-3.60	-3.60	-3.60
70170					-1.10	-1.10	-1.10			
70171		.39	.39	.39						
80036	UX DRA	.22	.22	.22	-.41	-.41	-.41			
80048	S CEP	-1.42	-1.64	-1.85	-2.91	-3.01	-3.11			
-10002	33 PSC	2.15	2.15	2.15						
-10006	IOT CET	.82	.82	.82	-.44	-.44	-.44			
-10035	U CET	2.25	2.25	2.25	1.41	1.41	1.41			
-10043	Z ERI	.35	.35	.35	-.84	-.84	-.84			
-10048	EPS ERI	1.43	1.42	1.40						
-10055	GAM ERI	-.82	-.82	-.82	-1.36	-1.36	-1.36			
-10064	OMI2 ERI	2.35	2.35	2.35						
-10083	R LEP	-.83	-.95	-1.06	-2.50	-2.52	-2.54	-2.06	-2.57	-2.92
-10085	RET ORI	.13	.13	.13	.03	.03	.03	-.52	-.55	-.57
-10093	H 42				-4.50	-4.50	-4.50	-5.00	-5.00	-5.00
-10098	KAP ORI	2.60	2.60	2.60						
-10169	PGC 1985	.19	-.11	-.35	.12	.12	.12	.13	.13	.13
-10194	FK HYA							-2.83	-2.83	-2.83
-10199	RY HYA				-.50	-.50	-.50			
-10217	ALF HYA	-1.22	-1.35	-1.46	-1.28	-1.28	-1.28			
-10242	U HYA	-1.10	-1.10	-1.10	-1.82	-1.82	-1.82			
-10253	DEL CRT	.77	.77	.77						

Table A1 (Cont.)

		4.2 MICRONS			11 MICRONS			19.8 MICRONS		
IRC	NAME	MAX	MEAN	MIN	MAX	MEAN	MIN	MAX	MEAN	MIN
-10274	PSI VIR	-.17	-.17	-.17						
-10286	ALF VIR	1.53	1.53	1.53	1.78	1.78	1.78	-1.44	-1.44	-1.44
-10288	74 VIR	.05	.05	.05						
-10290	S VIR	-.11	-.22	-.33	-1.29	-1.46	-1.60			
-10300	KAP VIR	.92	.92	.92						
-10329					-.50	-.50	-.50			
-10339	V OPH	1.51	1.22	.99	.33	.19	.06			
-10343	ZET OPH	2.61	2.61	2.61						
-10348		.55	.55	.55						
-10376	XX OPH	2.45	2.42	2.39	1.27	1.27	1.27			
-10381		.99	.85	.66	-1.14	-1.25	-1.40			
-10395		.89	.89	.89						
-10396		-.23	-.23	-.23	-1.48	-1.71	-1.90			
-10401					-1.00	-1.00	-1.00			
-10414					-2.20	-2.20	-2.20			
-10415	FR SCT	2.05	1.79	1.58	.70	.70	.70			
-10419	3,49	1.79	1.79	1.79						
-10422	UY SCT	.21	.21	.21	-1.50	-2.03	-2.39			
-10434		1.45	1.45	1.45	-.50	-.50	-.50			
-10435	BD-14-5105	1.13	1.13	1.13						
-10440		2.33	2.33	2.33						
-10441	6X SCT	.71	.71	.71	-.10	-.10	-.10			
-10445		2.28	2.28	2.28						
-10450		.64	.64	.64	-1.30	-1.40	-1.50			
-10461	P SCT	1.42	1.42	1.42	.40	.40	.40			
-10467	S SCT	.43	.43	.43	-.42	-.81	-1.10			
-10479	RW SCT	.68	.68	.68						
-10483	12 AQL	2.41	2.41	2.41						
-10486	V AQL	-.36	-.36	-.36	-1.48	-1.48	-1.48			
-10490	M 16	1.28	1.28	1.28	.50	.50	.50			
-10497	W AQL	-.83	-1.03	-1.20	-2.93	-3.02	-3.10			
-10502		-.04	-.04	-.04	-2.40	-2.40	-2.40			
-10524	GY AQL	-.25	-.25	-.25	-2.40	-2.56	-2.70			
-10529		-.55	-.55	-.55	-3.20	-3.20	-3.20			
-10534	ALF1 CAP	1.71	1.71	1.71						
-10535	ALF2 CAP	1.21	1.21	1.21						
-10537	BET CAP	.81	.81	.81						
-10548	3 AQR	-.27	-.36	-.43	-.33	-.33	-.33			
-10557	MUU AQR	2.14	2.14	2.14						
-10565	BET AQR				.34	.34	.34	-.04	-.04	-.04
-10608	30 PSC	-.55	-.55	-.55	-.36	-.36	-.36			
-10609	W CET	1.41	1.41	1.41						
-20084	17 LEP	.55	.55	.55	-1.37	-1.37	-1.37	-2.27	-2.27	-2.27
-20105	ALF CMA	-1.27	-1.33	-1.38	-1.30	-1.32	-1.33	-1.47	-1.47	-1.47
-20112	OMI1 CMA	.10	.10	.10	-.23	-.23	-.23			
-20173	AK HYA							-2.48	-2.48	-2.48
-20184		.64	.64	.64	.88	.88	.88			
-20197		.65	.65	.65	-2.10	-2.10	-2.10	-5.50	-5.50	-5.50
-20210	MUU HYA	.19	.19	.19						
-20217	MUU HYA	.10	.10	.10						
-20218	V HYA	-2.07	-2.09	-2.12	-3.90	-4.02	-4.12	-4.31	-4.41	-4.50
-20222	R CRT	-1.55	-1.55	-1.55	-2.70	-2.70	-2.70			
-20233	EPS CRV	-.10	-.10	-.10						
-20240	BET CRV	.61	.61	.61	.97	.97	.97			
-20242	T CRV	1.58	1.58	1.58	.10	-.20	-.44			

Table A1 (Cont.)

IRC	NAME	4.2 MICRONS MAX	4.2 MICRONS MEAN	4.2 MICRONS MIN	11 MICRONS MAX	11 MICRONS MEAN	11 MICRONS MIN	19.8 MICRONS MAX	19.8 MICRONS MEAN	19.8 MICRONS MIN
-20249	GAM HYA	.70	.70	.70						
-20254	R HYA	-2.97	-3.03	-3.20	-4.11	-4.39	-4.62	-4.51	-4.64	-4.76
-20266		.19	.19	.19	-.22	-.37	-.50			
-20275	BS 5568	2.66	2.43	2.24						
-20286	RS LIB	-.28	-.28	-.28	-1.69	-1.69	-1.69			
-20291	42 LIB	1.94	1.94	1.94						
-20296	THE LIB	1.37	1.37	1.37						
-20303	DEL SCO	2.87	2.87	2.87						
-20305	BET1 SCO	2.73	2.73	2.73						
-20318	PHI OPH	2.22	2.22	2.22						
-20322		.75	.75	.75						
-20411	HEE 42+43				-.20	-.20	-.20			
-20417	VE 2-45	-.58	-.62	-.66	-2.10	-2.20	-2.30			
-20421	GC 24547				-1.60	-1.60	-1.60			
-20423					-1.10	-1.10	-1.10			
-20424	1.232	-.72	-.87	-1.03	-3.10	-3.10	-3.10			
-20427					-1.40	-1.40	-1.40			
-20431	VX SGR	-1.62	-1.99	-2.32	-4.34	-4.76	-5.02	-5.43	-5.55	-5.60
-20434	AX SGR	2.56	2.49	2.40	-.32	-.51	-.68	-1.96	-1.96	-1.96
-20439					-2.00	-2.00	-2.00			
-20445		1.47	1.47	1.47						
-20451	14 SGR				-1.30	-1.30	-1.30			
-20445		1.47	1.47	1.47						
-20451	14 SGR				-1.30	-1.30	-1.30			
-20454					-2.30	-2.30	-2.30			
-20464		1.72	1.72	1.72						
-20466	N 6618				-6.43	-6.43	-6.43			
-20526	NU1 SGR	-1.56	-1.56	-1.56	-1.68	-1.68	-1.68			
-20527	UY SGR				-1.90	-1.90	-1.90			
-20528	NU2 SGR	1.82	1.82	1.82						
-20530	XI2 SGR	.78	.78	.78						
-20534	SU SGR	-.44	-.44	-.44	-1.90	-1.90	-1.90			
-20536	OMI SGR	1.39	1.39	1.39						
-20540		1.06	1.00	.95	-1.20	-1.67	-2.00			
-20542	PI SGR	1.67	1.67	1.67						
-20553	BS 7317	2.41	2.41	2.41						
-20554	V1942 SGR	.16	.16	.16						
-20558	UPS SGR	1.44	1.44	1.44	-.30	-1.29	-1.65			
-20568	AQ SGR	.66	.66	.66	-.49	-.49	-.49			
-20596	RS CAP				-.80	-.80	-.80			
-20602	ZET CAP	1.68	1.68	1.68						
-20604	36 CAP	2.30	2.30	2.30						
-20642	R AQR	-2.27	-2.27	-2.27	-4.46	-4.46	-4.46	-3.00	-4.07	-4.40
-30076	DEL CMA	.16	.16	.16	-.06	-.06	-.06			
-30087	VY CMA	-3.06	-3.34	-3.74	-6.00	-6.31	-6.60	-7.20	-7.58	-7.82
-30182	BS 4532	-.29	-.29	-.29	-.50	-.50	-.50			
-30207	W HYA	-3.41	-3.83	-4.05	-4.80	-5.23	-5.50	-5.20	-5.51	-5.75
-30213	PI HYA	.51	.51	.51						
-30217		1.03	1.03	1.03	-.79	-.79	-.79			
-30219		-2.22	-2.22	-2.22	-4.07	-4.07	-4.07			
-30228	SIG LIB	-1.37	-1.44	-1.50	-1.11	-1.39	-1.62	-2.25	-2.25	-2.25
-30231	2 LUP	1.93	1.93	1.93						
-30260	SIG SCO	2.05	2.05	2.05	1.66	1.66	1.66			
-30265	ALF SCO	-3.98	-3.99	-4.00	-4.60	-4.67	-4.73	-4.86	-4.88	-4.90
-30282	AH SCO				-3.20	-3.20	-3.20			

Table A1 (Cont.)

		4.2 MICRONS			11 MICRONS			19.8 MICRONS		
IRC	NAME	MAX	MEAN	MIN	MAX	MEAN	MIN	MAX	MEAN	MIN
-30267	CD30-13953				-1.10	-1.10	-1.10			
-30316					-1.80	-1.80	-1.80			
-30321	CAL CTR				-2.90	-2.90	-2.90			
-30326	KW SGR	.60	.60	.60	-1.90	-1.90	-1.90			
-30358	CD29-14520				-.10	-.10	-.10			
-30363	CD26-12859				-1.10	-1.10	-1.10			
-30398		-.41	-.73	-.97	-3.10	-3.29	-3.50			
-30192E	2 CEN	-1.65	-1.66	-1.68	-1.33	-1.64	-1.88			
-30287E	BS 6392	1.32	1.32	1.32	-.84	-.84	-.84			
-40314E	V MIC	.71	.71	.71	-1.48	-1.48	-1.48	-3.70	-3.70	-3.70
-40325E	DEL2 GRU	-.90	-.90	-.90	-1.00	-1.00	-1.00			
-50001E	R HOR	-2.21	-2.21	-2.21	-3.50	-3.50	-3.50	-3.94	-3.90	-3.90